



HAL
open science

Optical Analysis of Combustion and Soot Formation in a CI Engine Fuelled with Water in Diesel Emulsion through Microchannels Emulsification

C Tornatore, R Calabria, L Marchitto, J Belletre, P. Massoli, A. Montillet, G
Valentino

► To cite this version:

C Tornatore, R Calabria, L Marchitto, J Belletre, P. Massoli, et al.. Optical Analysis of Combustion and Soot Formation in a CI Engine Fuelled with Water in Diesel Emulsion through Microchannels Emulsification. *Journal of Physics: Conference Series*, 2018, Proceedings of the XXV A.I.V.E.L.A. Annual Meeting 9–10 November 2017, Rome, Italy, 1110, pp.012010. 10.1088/1742-6596/1110/1/012010 . hal-01969893

HAL Id: hal-01969893

<https://hal.science/hal-01969893>

Submitted on 21 Jul 2023

HAL is a multi-disciplinary open access archive for the deposit and dissemination of scientific research documents, whether they are published or not. The documents may come from teaching and research institutions in France or abroad, or from public or private research centers.

L'archive ouverte pluridisciplinaire **HAL**, est destinée au dépôt et à la diffusion de documents scientifiques de niveau recherche, publiés ou non, émanant des établissements d'enseignement et de recherche français ou étrangers, des laboratoires publics ou privés.

PAPER • OPEN ACCESS

Optical Analysis of Combustion and Soot Formation in a CI Engine Fuelled with Water in Diesel Emulsion through Microchannels Emulsification

To cite this article: C Tornatore *et al* 2018 *J. Phys.: Conf. Ser.* **1110** 012010

View the [article online](#) for updates and enhancements.

You may also like

- [Application of MDAG from Fully Hydrogenated Palm Kernel Oil on Making of Icing Sugar and Cake](#)
M Mursalin, S Sahrial and Y Yernisa
- [A decomposition method for the simultaneous reconstruction of temperature and soot volume fraction distributions in axisymmetric flames](#)
Huawei Liu, Huaichun Zhou and Chao Xu
- [Pickering emulsions: structure, properties and the use as colloidosomes and stimuli-responsive emulsions](#)
Marina Yu. Koroleva and Evgeny V. Yurtov

Optical Analysis of Combustion and Soot Formation in a CI Engine Fuelled with Water in Diesel Emulsion through Microchannels Emulsification

C Tornatore¹, R Calabria¹, L Marchitto¹, J Belletre², P Massoli¹, A Montillet³, G Valentino¹

¹ Istituto Motori CNR, Viale Marconi 8, 80125 Naples, Italy

² Université de Nantes, CNRS, LTN, UMR-6607, B.P. 50609, 44306 Nantes cedex 3, France

³ Université de Nantes, CNRS, GEPEA, UMR-6144, B.P. 406, 44602 Saint-Nazaire, France

l.marchitto@im.cnr.it

Abstract. Water in diesel emulsion (WiDE) is a viable solution for lowering both NO_x and Soot emissions from compression ignition (CI) engines. In this paper, the effect of WiDE on the combustion process and exhaust emissions of a prototype optically accessible CI engine was investigated through conventional in-cylinder pressure measurements and optical diagnostics. The emulsion (9.1%v of water) was produced through a prototype designed microchannels emulsifier with a small amount of nonionic surfactant. Commercial diesel was set as reference fuel and compared to WiDE. The start of injection (SOI) was swept from 8 to 23 CAD BTDC. For diesel fuel, the injected mass and injection pressure were representative of a medium load regime, WiDE injection interval was adjusted to keep constant the energy content. Compared to Diesel, WiDE induced an increase in ignition time, enhancing the air/fuel mixing with a simultaneous reduction in PM and NO_x. 2D chemiluminescent emission measurements highlighted a reduction in soot formation using WiDE, without significant changes in soot oxidation rate.

1. Introduction

Due to high fuel efficiency and specific power output, Compression Ignition (CI) engines still represent a probable solution to meet the new stringent regulations on CO₂ emission. However, this kind of internal combustion engines emits a high quantity of Nitrogen Oxides (NO_x) and Particulate Matter (PM) and it is necessary to find new reliable solutions for satisfying worldwide exhaust emissions regulation [1-5].

In recent times, great attention has been paid to water addition in IC engines to lower air-fuel charge temperature with benefits for NO_x and PM emissions. Water can be introduced using a separate injection system or by means of fuel as Water in Diesel Emulsion (WiDE) [6-8]. Water injection (WI) allows a simultaneous reduction in NO_x and PM emission: NO_x emission decreases due to in-cylinder temperature lowering and charge dilution; the larger induction time promotes a better air-fuel mixing, reducing the smoke. Compared to the emulsion, water injection allows changing the water-diesel ratio depending on the engine operative conditions. On the other hand, the complex engine design due to the introduction of a secondary injection system makes this solution expensive



and unfeasible. Moreover, a double injection system could lead to local too high water concentration region and impingement against the cylinder wall with risk of water dilution in the oil.

The usage of WiDE does not require any modification of the engine. Up to the present time, many aspects of WiDE have been studied, especially regarding diesel engine performance and the emission. The results from the scientific literature on this topic show a reduction in NO_x, smoke and fuel consumption over diesel fuel [9]. WiDE has been found to improve brake power, torque and thermal efficiency (BTE), compared to net Diesel at medium-high load in a wide range of engine speeds [10-13]. Compared to WI [7, 8], WiDE provides larger reduction in PM-NO_x emission, with further benefits on engine performance. While WI induces a lowering of fuel efficiency and of BTE due to the reduction in the charge temperature, WiDE provides a more efficient combustion even over net diesel fuel. The reason for this improvement should be ascribed to the micro-explosion phenomenon [10, 11, 14].

Microexplosion is the rapid breakup of emulsion droplets into smaller droplets due to the difference in the evaporation rates of diesel and water: water reaches the boiling point faster, destroying the diesel shell [15]. These microexplosions induce a fast break-up or secondary atomization of the fuel droplet, which, in turn, causes rapid fuel evaporation and, hence, leads to an improved air-fuel mixing. The atomization efficiency of droplets microexplosion depends on engine operating conditions [12] as well as on the emulsion structure [15]. The size distribution of the dispersed water droplets affects the BTE [16], NO_x emissions, smoke and unburned Hydrocarbons (UHC) [17, 18].

From a thermodynamic point of view, an emulsion is an unstable system and this turns out to be a serious drawback. Instability of emulsions leads to floating of droplets to the surface, cohesion between droplets, and finally to creaming and separation. To prevent this phenomenon, surfactants have been widely used but they can favor the raise of sludge and cause the wear of the engine components. With this aim, emulsifier technology, capable to produce the fuel emulsion on board, right before the injection, can overcome stability issues without the use of additives [19, 20].

This paper reports the results of an experimental activity carried on WiDE (9.1%v water concentration) produced through an especially designed microchannels emulsifier [21] and injected in a prototype single cylinder high swirl CI engine, equipped with a common rail injection system.

Thermodynamic analysis was performed and exhaust pollutant were measured at the exhaust. Combustion digital imaging was applied in the optically accessible combustion chamber: more in details, 2D chemiluminescence was detected through flame emission filtering at 690 nm to follow the soot evolution. The aim of the paper is to fill the scientific knowledge lack on the effect of WiDE on combustion in a real engine system.

2. Experimental set-up and procedure

2.1. Microchannels Emulsification

An especially designed microchannels emulsifier, shown in figure 1, was used to produce the emulsion [21]. Two pumping systems supply controlled flows of water and diesel fuel to the emulsifier. In particular, a double piston displacement pump (ARMEN - APF-100-251) is used for water and two turbo-pumps arranged in series for diesel fuel. Diesel flow rate can reach values higher than 300 ml/min with a pressure drop of 0.4 MPa.

Pressure sensors (measuring range between 0 and 2.5 MPa and accuracy of $\pm 0.25\%$ of full scale) allow a precise control of flow rate between the pump and the inlet of the microchannels. The sensors measure the relative and static pressure for each of the two mixed phases. Connections between pumps and microchannels are made using Fluorinated Ethylene Propylene (FEP) tubes with an inner diameter of 1.55 mm and an outer diameter of 3.125 mm.

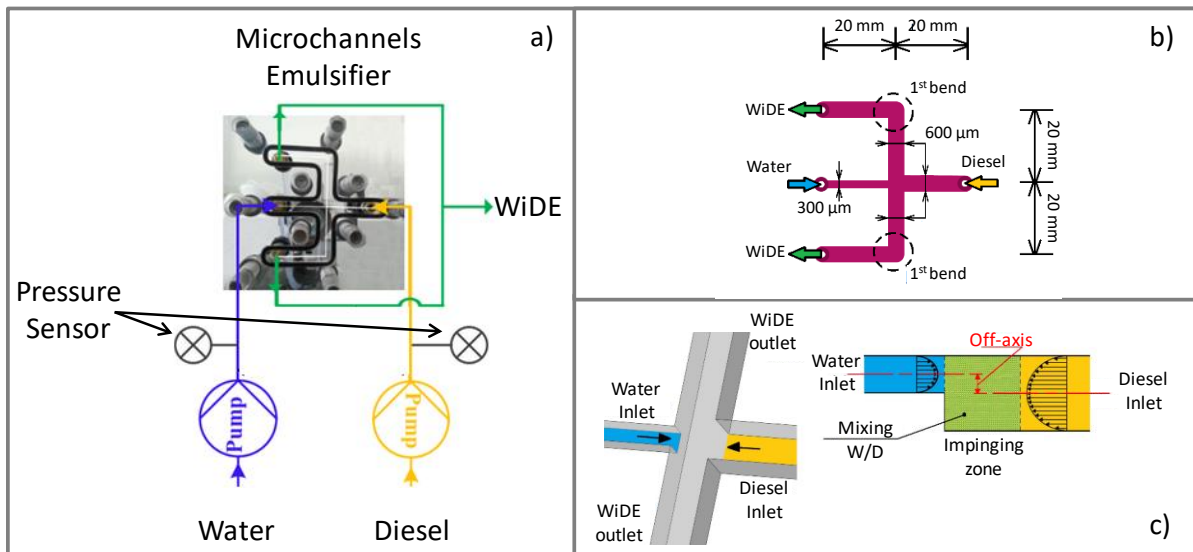


Figure 1. a) Emulsification set-up, b) schematic of Microchannels Emulsifier c) sketch of Water/Diesel impinging zone.

A sketch of microchannels in the emulsifier is shown in figure 1 b): two square cross section crossing microchannels allow two separate inlets for Diesel and water and two WiDE outlets. Diesel and emulsion channels cross section sizes are $600\ \mu\text{m} \times 600\ \mu\text{m}$, while the water one is $300\ \mu\text{m} \times 300\ \mu\text{m}$. As shown in Figure 1 c), water and Diesel are forced to impact head-on, with a slight misalignment to promote a swirl flow in the impingement zone. This kind of emulsifier has been developed to comply with required characteristics of WiDE (mean diameter of droplet $\sim 4\ \mu\text{m}$, narrow size distribution, water fraction smaller than $\sim 10\%$). Further details about WiDE procedure can be found in [21].

This system allows producing an emulsion suitable for immediate use without additives, anyway a small amount (0,2%v) of nonionic surfactant (SPAN80) was added in order to store the emulsion. For this work, the water concentration in WiDE was 9.1%v.

2.2. Engine Test Bench and Optical Diagnostic Experiments

The experiments were carried out in a single cylinder 2-stroke compression ignition engine, sketched in Figure 2. An external high swirl optically accessible combustion bowl (diameter: 50 mm and depth: 30 mm), equipped with a high-pressure common rail injection system, is connected to the main cylinder through a tangential duct. The engine runs at the fixed speed of 500 rpm. Compressed air flow is forced within the combustion bowl when the piston approaches Top Dead Centre (TDC). As a result, a counter clockwise swirl flow is obtained, reproducing a fluid dynamic environment similar to a real light duty direct injection diesel engine, with the rotation axis coincident to the symmetry axis of the chamber. Further engine specifications can be found in [22].

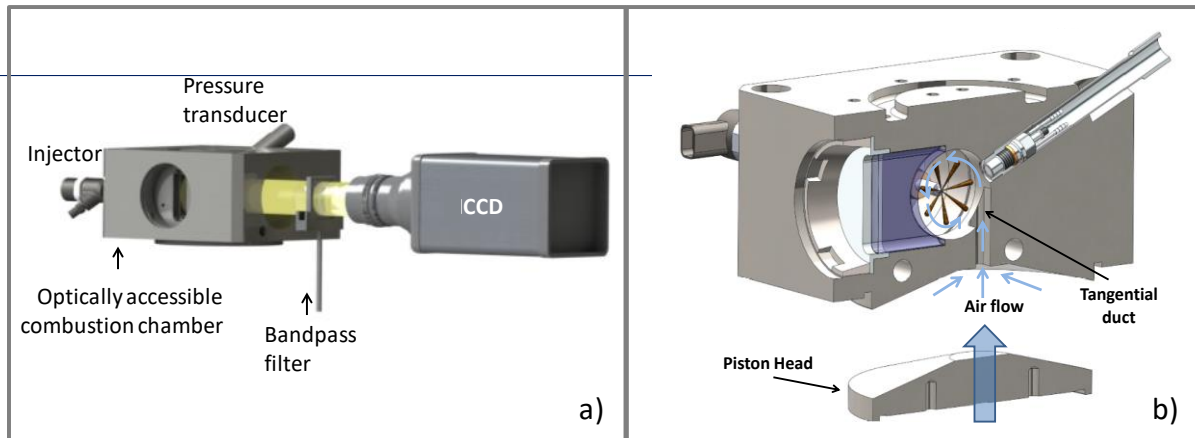


Figure 2. Sketch of the optically accessible engine (a) and cross section of the optically accessible combustion chamber (b).

The nozzle is mounted within the combustion bowl, with its axis coincident to the chamber axis. The fuel is sprayed within the swirling air motion and the combustion process mainly develops within the chamber. After TDC, as the piston moves downward, the flow reverses its motion and hot gases flow through the tangential duct to the cylinder and finally to exhaust ports. The combustion chamber is equipped with a circular shaped (50 mm diameter) optical window, in front of the injector, used to collect images. A common rail injection system supplies fuel to a solenoid-controlled injector, located on the opposite side of the circular optical access. The nozzle is a micro-sac 7 hole, 0.136 mm diameter, 148° spray angle nozzle. An external roots blower provides an intake air pressure of 0.107 MPa with a peak pressure within the combustion chamber of 4.3 MPa under motored conditions. A crank angle encoder signal synchronized the camera acquisitions and the engine, through a delay unit. The AVL Indimodul recorded the Transistor-Transistor Logic (TTL) signal to monitor optical acquisitions, the current signal from injector solenoid and the in-cylinder pressure trace. Results of the in-cylinder pressure, acquired by a piezo-quartz transducer, were computed averaging 200 consecutive engine cycles. Exhaust gaseous emissions were acquired by the AVL DiGas 4000 analyzer for NO_x (1 ppm resolution). Smoke was measured by a part flow Opacimeter (AVL 439); the opacity was correlated to the PM concentration through an empirical formula [23].

Tests were carried out comparing combustion and emissions of the reference commercial diesel fuel to the WiDE ones. Considering the water inert for combustion, the comparison was done by fixing the quantity of diesel fuel injected. A single injection strategy was chosen, and the start of injection (SOI) was swept from 23 to 8 Crank Angle Degree before the TDC (CAD BTDC) with a step of 3 CADs. For the diesel case, the whole amount of injected fuel and injection pressure were set at 22 mg/str and 80 MPa, respectively, corresponding to a medium load regime for an automotive light duty diesel engine. For any investigated fuel and operating point, engine tests were carried out changing the injection interval to achieve the same chemical energy as the reference diesel (935 J/str).

2D chemiluminescent emission measurements, during the whole combustion process, were carried out using a Charge-Coupled Device (CCD) camera (pco.2000) coupled with a band-pass filter, centered at 690 nm, to discriminate the soot emission from other excited chemical species contribution in the visible wavelength range as CH and C₂ [23].

The high transmission (85%) and small width (12 nm FWHM) of the band-pass filter allowed to separate the soot emission from other excited species [24].

2.3. WiDE characterization

The structure of WiDE was investigated by means of an optical microscope (Olympus BX51), allowing to get information about the size distribution of water droplets inside the diesel matrix. Three different samples were collected in order to estimate the emulsion quality and stability: the first one, immediately after the emulsification process (fresh WiDE), the second one was aged for 24 hours at room temperature (about 20°C), while the last one was circulated in the common rail system under low/high pressures loop condition (0.04MPa/150MPa), for two hours. An example of micrograph referring to the fresh WiDE is shown in figure 3a).

The micrographs were analyzed through ImageJ, a Java-based image processing software. A droplets counting and sizing procedure was applied to compare the diameter distribution of the three WiDE samples. The results are shown in figure 3 b). For each investigated sample, the size range is quite narrow, with a peak between 1 and 2 μm . A slight growth in the size was found when aging the WiDE, a further increase was found after the low/high pressures loop. As general remark, the emulsion can be considered stable and its breakdown after aging is not significant with a fine size distribution of the dispersed phase even after tests in the common rail pumping circuit.

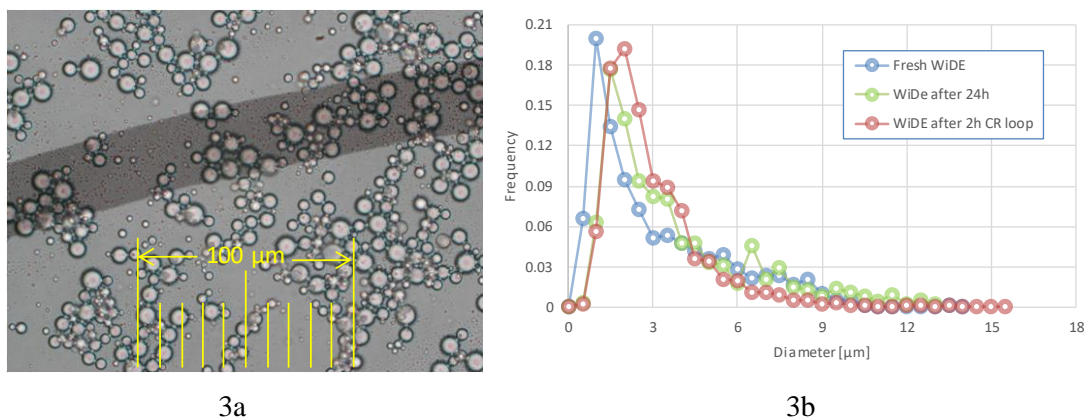


Figure 3. Fresh WiDE emulsion micrograph (a) and size distribution histogram of the three WiDE samples (b).

A quantitative comparison of the three distributions was performed by estimating the area A0.5-4.5, defined as the count of droplets in the range of diameters between 0.5 μm and 4.5 μm . The area A0.5-4.5 represented the 65% of the area representative of the total droplets population for the three samples. This indicates a very fine dispersion of the water phase. The water droplets histogram of the fresh emulsion (blue curve) shows an A0.5-4.5 of about 72% and a modal value of 1.5 μm . This value increases to 2.0 μm for the aged 24 hours WiDE (green curve), showing a very limited water droplets coalescence. A narrower distribution was found when WiDE was circulated in the common rail system under low/high pressures loop condition (red curve) if compared to the fresh WiDE, with A0.5-4.5 =82.9% and a modal size of the dispersion phase of 2.5 μm .

3. Engine tests

In the preliminary part of the experimental activity, engine tests were carried out to estimate the effect of start of injection (SOI) and fuel on performance and emissions. Figure 4 shows the in-cylinder pressure traces for Diesel (a) and WiDE (b) combustion, for all the investigated injection timing. Early SOIs induce early start of combustion (SOC) and, as the injection timing is advanced, the pressure peak increases. For each test case the emulsion provides a stable combustion pressure curve with a behavior similar to diesel, except for the increase in air-fuel mixture ignition time.

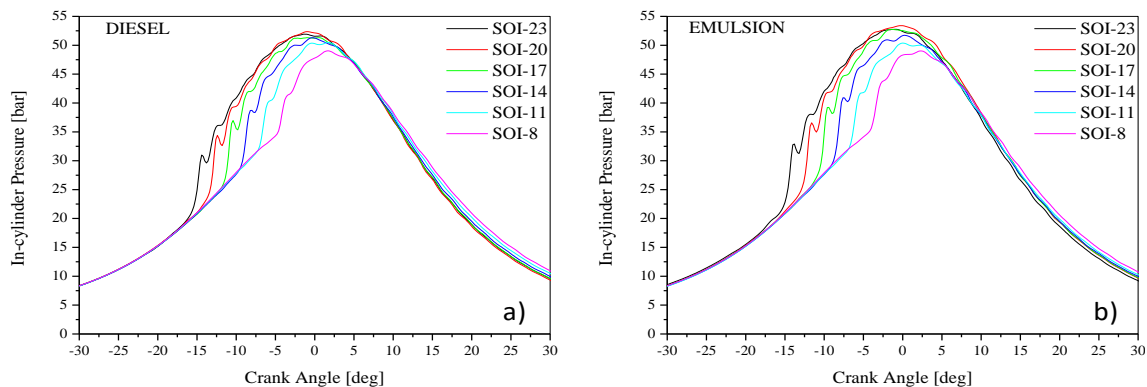


Figure 4. Pressure trace for diesel (a) and WiDE (b) at different starts of injection.

Figure 5 reports the ignition delay (ID) (a) and maximum in-cylinder pressure (b). The ID is obtained as the difference in CAD between the electronic start of injection and the SOC, defined as the relative maximum of the pressure trace first derivative. In order to operate at the same fuel chemical energy content for both fuels, the injection duration was set at 2.6 and 2.7 CAD for Diesel and WiDE, respectively. The minimum ID evaluated is 3.8 CAD at SOI=8 CAD BTDC for Diesel fuel. This means that, for every operative condition, the injection can be considered complete before the SOC. For both fuels, a rise in ID is recorded by advancing the injection, with a maximum value of about 8.75 CAD at SOI=23 CAD BTDC for WiDE. An almost constant ID increase versus start of injection of about 0.7 CAD can be observed switching from diesel to emulsion. The larger ignition time, due to the lower temperature caused by water evaporation, results in an increase in the amount of fuel burned during the premixed phase, with a consequent increment in pressure peak (figure 5 b). When retarding the SOI, a slight decrease in in-cylinder pressure maximum is found and the different behavior between Diesel and WiDE is reduced.

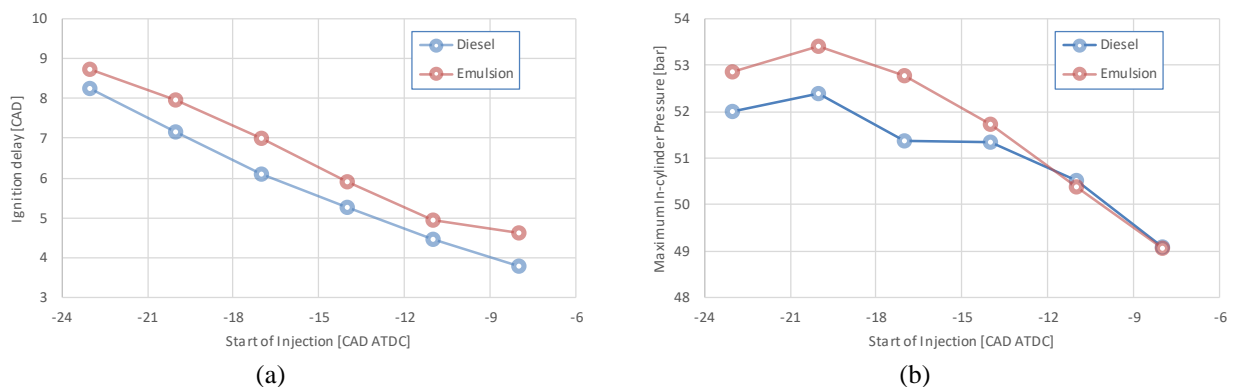


Figure 5. Effect of WiDE on Ignition Delay (a) and Pressure Peak (b).

Figure 6 shows NO_x-soot trade-off for all investigated test conditions: the behavior is the typical one for diesel combustion emissions. In fact, at the earliest SOIs the soot production is negligible for both fuels until 14 CAD BTDC SOI, while a NO_x maximum of 146 ppm is obtained for Diesel at the most advanced injection timing (23 CAD BTDC). The WiDE combustion, even though displays a similar behavior, strongly reduces both NO_x and soot emissions.

In agreement with results reported in the scientific literature [7], emulsion is very effective in reducing NO_x levels. This can be explained as follows: water evaporation reduces local temperatures in the spray, including those of zones where NO is produced (on the lean side of the diffusion flame during injection and in the combustion products after the end of injection). This results in a NO

production rate decrease [25]. Moreover, for a given mass of burned fuel, the heat is released in a higher mass of gas (because of the dilution of the fuel by water). As a result, the dilution by water has a positive local thermal effect on NO reduction. In addition, Miyauchi et al. [26] reported that the presence of water can form OH radicals: this promotes the oxidation of hydrocarbon fragments and the reduction in NO levels.

As regards PM emission, the larger ID, due to the water content, reduced the locally rich fuel/air mixture regions in which the soot is produced. Moreover, WiDE injection strategies induced an increase in air entrainment per unit of diesel-fuel mass; this effect results in a decrease of PM emission. The best compromise for NO_x-soot, intended as the cross of soot and NO_x curves, was obtained close to 11 CAD BTDC, while the injection timing at SOI=14 CAD BTDC was the latest case characterized by close to zero soot emission (~1.5 mg/m³ for WiDE). For this reason, these two injection timings were selected as reference test conditions for the optical investigation.

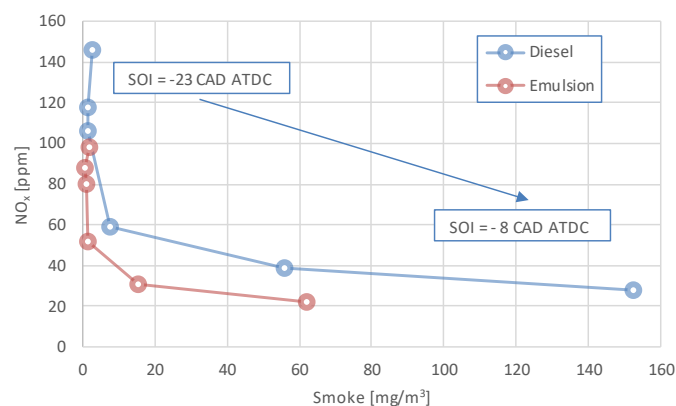


Figure 6. Effect of WiDE on PM-NO_x trade-off.

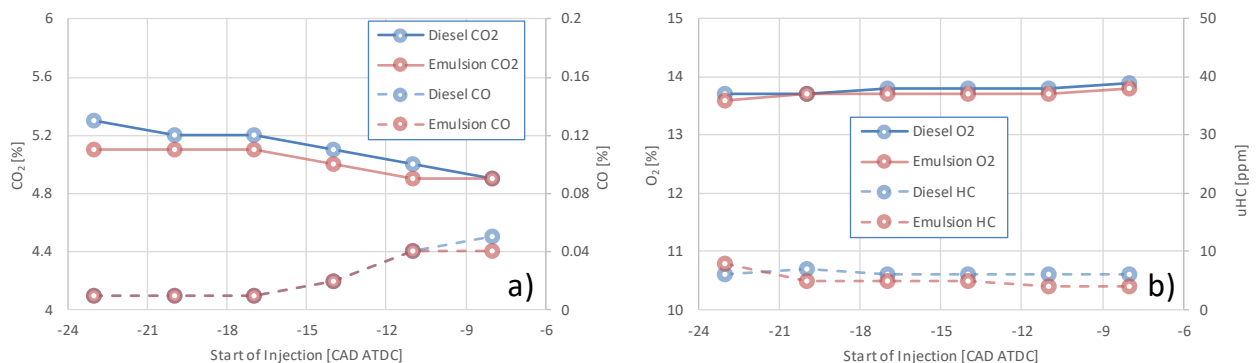


Figure 7. Effect of WiDE on CO and CO₂ (a) and on O₂ uHC (b) exhaust emission.

Figure 7 a) shows the CO and CO₂ exhaust emissions versus the Start of Injection for both investigated fuel. As concerns CO₂, the trends measured for diesel and WiDE are very close, with emulsion a little bit below the diesel one. The maximum difference is of 0.2% at -23 CAD ATDC. Such a difference, even low, should be attributed to the different combustion phasing due to the increase in ignition delay when the engine is fueled with emulsion. As expected CO emission is close to zero for both fuels, due to the high air excess typical of compression ignition engines. The CO emission is always below 0.05 % suggesting that the use of emulsion does not result in a worsening of combustion. Figure 7 b) refers to the O₂ and unburned hydrocarbon (uHC) levels. The combustion is characterized by high oxygen content at the exhaust, with a trend almost constant versus the injection timing without significant variation when switching from Diesel to WiDE. As expected the high

oxygen content results in an almost negligible uHC emission (below 10 ppm) for Diesel. The introduction of water in the cylinder does not lead to a worsening of the combustion as the water is finely dispersed in the diesel matrix and it quickly evaporates. As a result, the uHC emission is close to zero as for the reference case.

Optical diagnostics have been applied in the combustion chamber in order to better understand the differences among the two fuels during the combustion process. More in details the combustion luminosity is acquired through an intensified CCD camera coupled to a bandpass filter centered at 690 nm. In this way, only the emission signal of soot is detected. The images have been post processed using ImageJ software. In particular, for each image the mean gray value and the center of mass position are obtained. The mean gray value is the average gray value obtained as the sum of the gray values of all the pixels in the image divided by the number of pixels. The Center of Mass (CoM) is the brightness-weighted average of the x and y coordinates of all pixels in the image. Connecting two consecutive points of the CoM trajectory, displacement vectors are obtained: they are able to show the direction and distance traveled with a straight line.

Figure 8 reports a sequence of images acquired for the two fuels and the two selected start of injection (11 CAD BTDC_lower sequences and 14 CAD BTDC_upper sequences), from the first significant luminous signal until the end of combustion. The flame is centered on the symmetry axis of the chamber, coincident with the injector axis. The spatial distribution of luminous signal highlights the swirl motion within the chamber, generated during the compression stroke by the tangential duct connecting the optically accessible combustion chamber to the main cylinder.

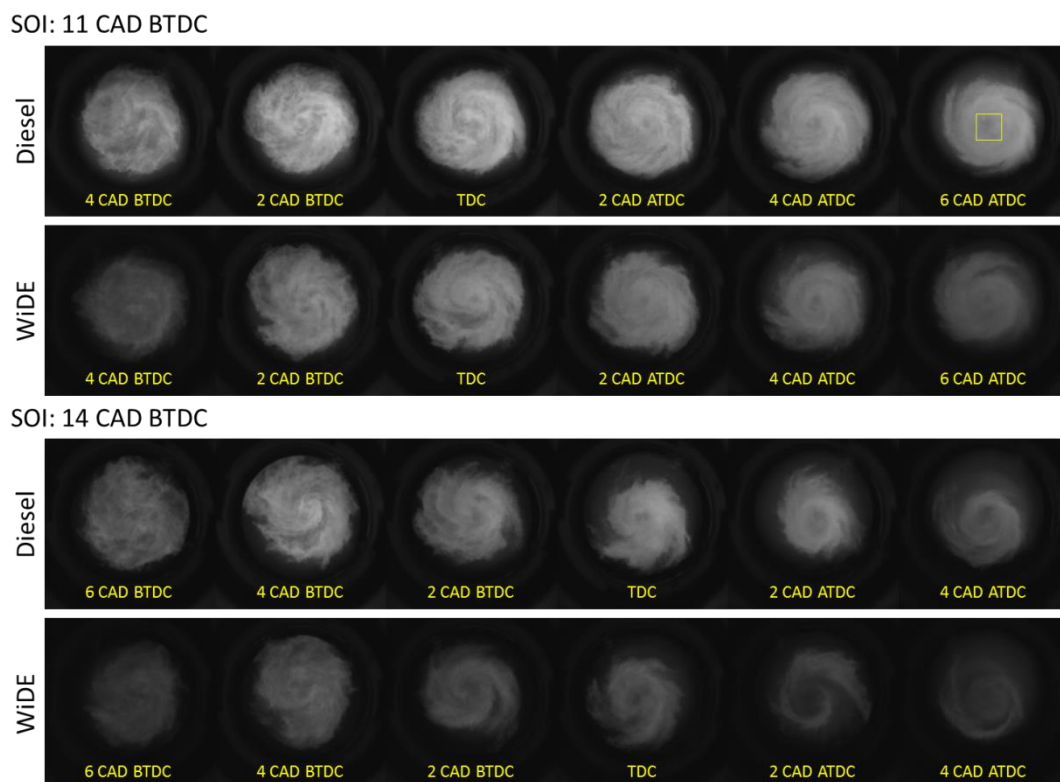


Figure 8. Soot emission visualization for diesel and WiDE at SOI= 11 CAD BTDC (upper) and 14 CAD BTDC (lower).

At 11 CAD BTDC SOI (figure 8_upper), the Diesel combustion luminosity increases due to the soot formation, up to a maximum at around TDC, followed by an intensity reduction due to the soot oxidation. Immediately after the TDC, the swirl air flow reverses pushing the hot gases toward the

tangential duct to the cylinder. As a consequence, the flame region quickly reduces. At 14 CAD BTDC SOI (figure 8 lower), the combustion starts some CADs before; the luminosity maximum is around 4 CAD BTDC. Compared to the later start of injection, the lower luminous signal is indicative of lower soot mass formation. Similarly, for both SOIs, the Diesel combustion is featured by higher luminous signal pointing out a strong soot reduction when switching to WiDE combustion.

Figure 9 reports the trajectory traced by the CoM in a zoomed area corresponding to the square in figure 8 (up - right). As shown, at SOI=14 CAD BTDC the center of mass moves with a counter clockwise motion and its path is wider if compared to the condition SOI=11 CAD BTDC.

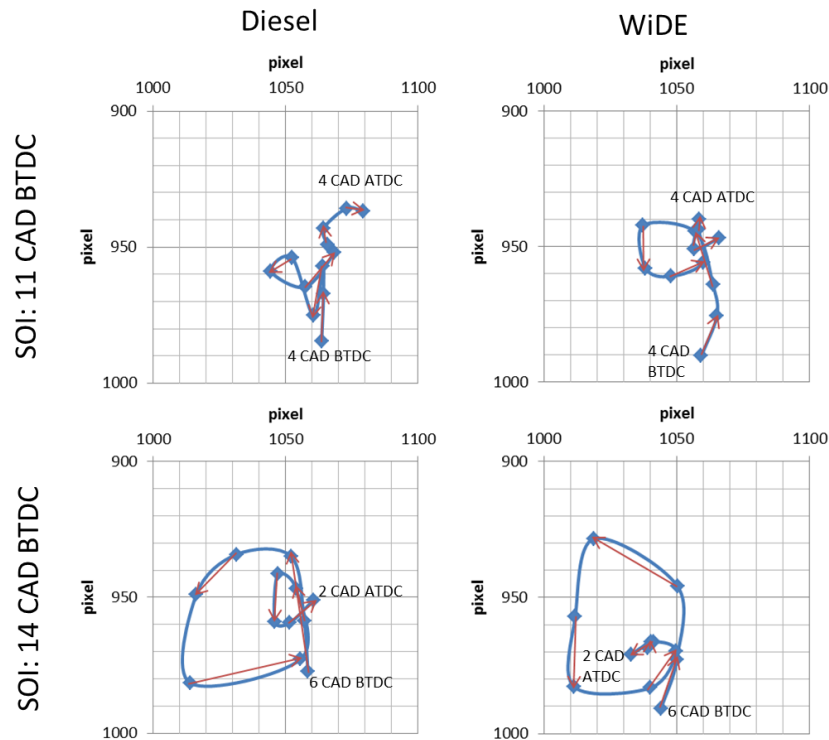


Figure 9. Center of mass trajectory in a zoomed area corresponding to the square reported in Figure 7 at SOI= 11 CAD BTDC (upper) and 14 CAD BTDC (lower).

At a fixed SOI, the trajectory is very similar for both fuels: it indicates that this parameter is mainly influenced by the fluid dynamic in the combustion chamber rather than by the fuel properties.

To easily follow the soot formation mechanism, the average gray value has been obtained for each image. The results are shown in figure 10: the plots refer to the average ensemble over 10 acquisitions. For both fuels and SOIs, the profile is characterized by a first linear increasing tendency due to the soot formation up to a maximum followed by a linear decreasing trend, due to the oxidation. The emulsion induces a strong reduction in soot formation at both investigated SOIs, while the soot oxidation rate is almost the same.

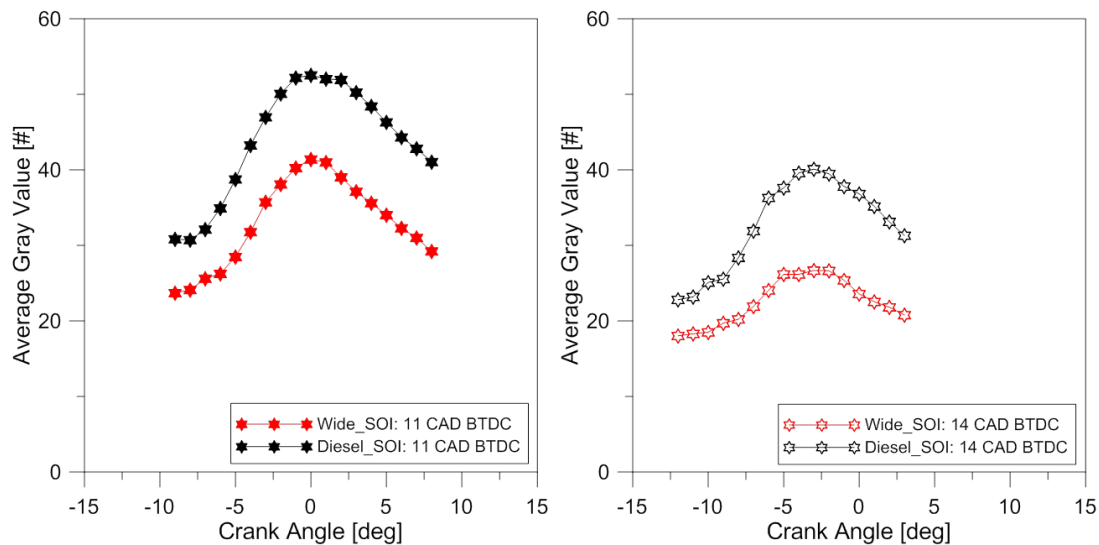


Figure 10. Evolution of soot average gray value at SOI= 11 CAD BTDC (left) and 14 CAD BTDC (right).

4. Conclusions

2D chemiluminescent emission measurements were carried out in a prototype optically accessible CI engine, fuelled with water in diesel emulsion (WiDE), to investigate the combustion process evolution and exhaust emissions. A band-pass filter, centered at 690 nm, was applied to discriminate the soot evolution. Engine tests were performed by comparing combustion and exhaust emissions of the reference commercial diesel to the WiDE. A prototype specifically designed microchannels emulsifier was used to produce WiDE; a small amount (0,2%v) of nonionic surfactant (SPAN80) was added to stabilize the emulsion.

The WiDE formed by means of the microchannels system resulted stable and the dispersed water phase showed a very fine size distribution with a narrow shape even after running into the high pressure common rail system.

Engine tests highlighted an increase in the ignition delay with the WiDE compared to the diesel fuel, resulting in a better air/fuel mixing with a reduction both in PM and NO_x.

The flame emission of Diesel combustion exhibited higher luminosity compared to the WiDE combustion, indicative of a greater soot mass formation.

The water emulsion lowered the soot formation process while the soot oxidation rate was not affected, as demonstrated by the spatially integrated luminosity, computed over the whole combustion image.

In conclusion, the experimental activity demonstrated the efficacy of the prototype microchannels emulsifier to produce stable WiDE, reducing engine PM and NO_x emissions, without penalties on performance. Further development of the prototype emulsifier will be aimed at using this device inline in the engine to avoid the use of surfactants, currently necessary to face the issues associated to WiDE storage.

References

- [1] W. Tutak, K. Lukács, S. Szwaja, Á. Bereczky, Alcohol–diesel fuel combustion in the compression ignition engine, *Fuel* 154 (2015) 196-206.
- [2] B. Yang, M. Yao, W.K. Cheng, Y. Li, Z. Zheng, S. Li, Experimental and numerical study on different dual-fuel combustion modes fuelled with gasoline and diesel, *Appl Energy* 113 (2014) 722-733.
- [3] A.K. Agarwal, D.K. Srivastava, A. Dhar, R.K. Maurya, P.C. Shukla, A.P. Singh, Effect of fuel

- injection timing and pressure on combustion, emissions and performance characteristics of a single cylinder diesel engine, *Fuel* 111 (2013) 374-383.
- [4] S. Roy, R. Banerjee, P.K. Bose, Performance and exhaust emissions prediction of a CRDI assisted single cylinder diesel engine coupled with EGR using artificial neural network, *Appl Energy* 119 (2014) 330-340.
- [5] K. Mathivanan, J.M. Mallikarjuna, A. Ramesh, Influence of multiple fuel injection strategies on performance and combustion characteristics of a diesel fuelled HCCI engine—An experimental investigation, *Exp Therm Fluid Sci* 77 (2016) 337-346.
- [6] M.S. Kumar, J. Bellettre, M. Tazerout, The use of biofuel emulsions as fuel for diesel engines: a review, *P I Mech Eng A-J Pow* 223 (7) (2009) 729-742.
- [7] K.A. Subramanian, A comparison of water–diesel emulsion and timed injection of water into the intake manifold of a diesel engine for simultaneous control of NO and smoke emissions, *Energy Conversion and Management*, 52 (2) (2011) 849-857.
- [8] Z. Şahin, M. Tuti, O. Durgun, Experimental investigation of the effects of water adding to the intake air on the engine performance and exhaust emissions in a DI automotive diesel engine, *Fuel* 115 (2014) 884-895.
- [9] T. Murayama, M. Tsukahara, Y. Morishima, N. Miyamoto, Experimental Reduction of NO_x, Smoke, and BSFC in a Diesel Engine Using Uniquely Produced Water (0-80%) to Fuel Emulsion, SAE Technical Paper 780224 (1978).
- [10] A.M. Ithnin, H. Noge, H.A. Kadir, W. Jazair, An overview of utilizing water-in-diesel emulsion fuel in diesel engine and its potential research study, *J Energy Inst* 87 (4) (2014) 273-288.
- [11] B.K. Debnath, U.K. Saha, N. Sahoo, A comprehensive review on the application of emulsions as an alternative fuel for diesel engines, *Renew Sust Energ Rev* 42 (2015) 196-211.
- [12] E. Yilmaz, H. Solmaz, S. Polat, A. Uyumaz, F. Şahin, M.S. Salman, Preparation of diesel emulsion using auxiliary emulsifier mono ethylene glycol and utilization in a turbocharged diesel engine, *Energ Convers Manage* 86 (2014) 973-980.
- [13] A. Alahmer, Influence of using emulsified diesel fuel on the performance and pollutants emitted from diesel engine, *Energ Convers Manage* 73(2013) 361-369.
- [14] M.Y. Khan, Z.A Abdul Karim, A.R.A. Aziz, I.M. Tan, Experimental Investigation of Microexplosion Occurrence in Water in Diesel Emulsion Droplets during the Leidenfrost Effect, *Energ Fuel* 28 (11) (2014) 7079-7084.
- [15] E. Mura, R. Calabria, V. Califano, P. Massoli, J. Bellettre, Emulsion droplet micro-explosion: Analysis of two experimental approaches, *Exp Therm Fluid Sci* 56.(2014) 69-74.
- [16] W.M. Yang, H. An, S.K. Chou, S. Vedharaji, R. Vallinagam, M. Balaji, K.J.E Chua, Emulsion fuel with novel nano-organic additives for diesel engine application, *Fuel* 104 (2013) 726-731.
- [17] Ali M.A.Attia, A.R. Kulchitskiy Influence of the structure of water-in-fuel emulsion on diesel engine performance, *Fuel* 116 (2014) 703-708.
- [18] A.K. Hasannuddin, J.Y. Wira, S. Sarah, M.I. Ahmad, S.A. Aizam, M.A.B. Aiman, S. Watanabe, N. Hirofumi, M.A. Azrina, Durability studies of single cylinder diesel engine running on emulsion fuel, *Energy* 94 (2016) 557-568.
- [19] N.A. Ramlan, W.J. Yahya, A.M. Ithnin, A.K. Hasannuddin, S.A Norazni, N.A. Mazlan, T. Koga, Performance and emissions of light-duty diesel vehicle fuelled with non-surfactant low grade diesel emulsion compared with a high grade diesel in Malaysia, *Energ Convers Manage* 130 (2016) 192-199.
- [20] A. Belkadi, D. Tarlet, A. Montillet, J. Bellettre, P. Massoli, Study of two impinging flow micro-systems arranged in series. Application to emulsified biofuel production, *Fuel* 170 (2016) 185-196.
- [21] J. Bellettre, A. Belkadi, A. Montillet, Device and method for carrying out continuous emulsion of two immiscible liquids World Patent WO2017103498 A1 (2017).
- [22] F. Corcione, G. Valentino, C. Tornatore, S. Merola, L. Marchitto, Optical investigation of

- premixed low-temperature combustion of lighter fuel blends in compression ignition engines, SAE Technical Paper2011-24-0045 (2011).
- [23] M. Lapuerta, F.J. Martos, M.D. Cárdenas, Determination of light extinction efficiency of diesel soot from smoke opacity measurements, *Meas Sci Technol* 16(10) (2005) 2048-2055.
- [24] H. Zhao, N. Ladommatos, Optical diagnostics for soot and temperature measurement in diesel engines, *Prog Energ Combust* 24 (3) (1998) 221-255.
- [25] A. Maiboom, X. Tazua, NO_x and PM emissions reduction on an automotive HSDI Diesel engine with water-in-diesel emulsion and EGR: An experimental study. *Fuel* 90 (2011) 3179-3192.
- [26] T. Miyauchi, Y. Mori, T. Yamaguchi, Effect of steam addition on NO formation, *Symp. (Int.) Combust.* 15 18 (1) (1981) 43-51.